The Meteoritical Society

Meteoritics & Planetary Science 43, Nr 7, 1127–1136 (2008)
Abstract available online at http://meteoritics.org

In situ micro-Raman and X-ray diffraction study of diamonds and petrology of the new ureilite UAE 001 from the United Arab Emirates

Dominik C. HEZEL[1, 2*], Leonid DUBROVINSKY[3], Lutz NASDALA[4, 5], Jean CAUZID[6], Alexandre SIMIONOVICI[7], Marko GELLISSEN[1], and Thorbjörn SCHÖNBECK[1]

[1]Universität zu Köln, Institut für Geologie und Mineralogie, Zülpicherstr. 49b, D-50674 Köln, Germany
[2]Present address: Department of Mineralogy, Natural History Museum, Cromwell Road, London, SW7 5BD, UK
[3]Bayerisches Geoinstitut, Universität Bayreuth, D-95440 Bayreuth, Germany
[6]ESRF, 6 rue Jules Horowitz, BP220, 38043 Grenoble Cedex, France
[4]Johannes Gutenberg-Universität Mainz, Institut für Geowissenschaften, Becherweg 21, D-55099 Mainz, Germany
[5]Present address: Universität Wien, Institut für Mineralogie und Kristallographie, Althanstraße 14, A-1090 Wien, Austria
[7]Laboratoire de Géophysique Interne et Tectonophysique, OSUG, BP 53, 38041 Grenoble, France
[*]Corresponding author. E-mail: d.hezel@nhm.ac.uk

(Submitted 16 June 2006; revision accepted 05 February 2008)

Abstract–A new olivine-pigeonite ureilite containing abundant diamonds and graphite was found in the United Arab Emirates. This is the first report of a meteorite in this country. The sample is heavily altered, of medium shock level, and has a total weight of 155 g. Bulk rock, olivine ($Fo_{79.8–81.8}$) and pyroxene ($En_{73.9–75.2}$, $Fs_{15.5–16.9}$, $Wo_{8.8–9.5}$) compositions are typical of ureilites. Olivine rims are reduced with Fo increasing up to $Fo_{96.1–96.8}$. Metal in these rims is completely altered to Fe-hydroxide during terrestrial weathering. We studied diamond and graphite using micro-Raman and in situ synchrotron X-ray diffraction. The main diamond Raman band (LO=TO mode at ~1332 cm^{-1}) is broadened when compared to well-ordered diamond single crystals. Full widths at half maximum (FWHM) values scatter around 7 cm^{-1}. These values resemble FWHM values obtained from chemical vapor deposition (CVD) diamond. In situ XRD measurements show that diamonds have large grain sizes, up to >5 μm. Some of the graphite measured is compressed graphite. We explore the possibilities of CVD versus impact shock origin of diamonds and conclude that a shock origin is much more plausible. The broadening of the Raman bands might be explained by prolonged shock pressure resulting in a transitional Raman signal between experimentally shock-produced and natural diamonds.

INTRODUCTION

A single stone of 155 g, completely covered by fusion crust was found during an archeological field trip in January 2005 on a parking site by H. Kallweit and R. Cuttler (Fig. 1). Officials were informed about this first finding of a meteorite in the United Arab Emirates (UAE). The meteorite was classified as an ureilite by D. C. Hezel and named United Arab Emirates 001 (UAE 001). The classification and initial description is published in the Meteoritical Bulletin No. 91 (Connolly et al. 2007; Hezel et al. 2006). The main mass and one thin section of the meteorite are located at Abu Dhabi Islands Archaeological Survey, ADIAS, PO Box 45553, Abu Dhabi, United Arab Emirates. The type specimen and one thin section are on deposit at Universität zu Köln, Institut für Geologie und Mineralogie, Zülpicher Straße 49 b, 50674 Köln, Germany.

Ureilites are ultramafic rocks generally thought to represent mantle residues, as is evident from depletion in incompatible elements. Typical modal major mineralogy of ureilites is olivine and pigeonite. Less than 10% is C-rich material interstitial to the silicates. Graphite is the dominant C-species and can reach mm-size. Most ureilites contain diamond that occurs within the graphite. A small group of ureilites, often referred to as "polymict," contains additional feldspar and other exotic components. Ureilites have some so far unexplained primitive characteristics. Their O-isotopes exhibit a large scatter and plot close to a slope 1 line in an oxygen 3-isotope-plot, in contrast to a mass-dependent fractionation line of slope ~0.51 that is usually observed in differentiated rocks (e.g., Mittlefehldt 2004 and references therein).

The origin of diamond in ureilites is still a matter of debate. Two competing theories exist: 1) In the canonical

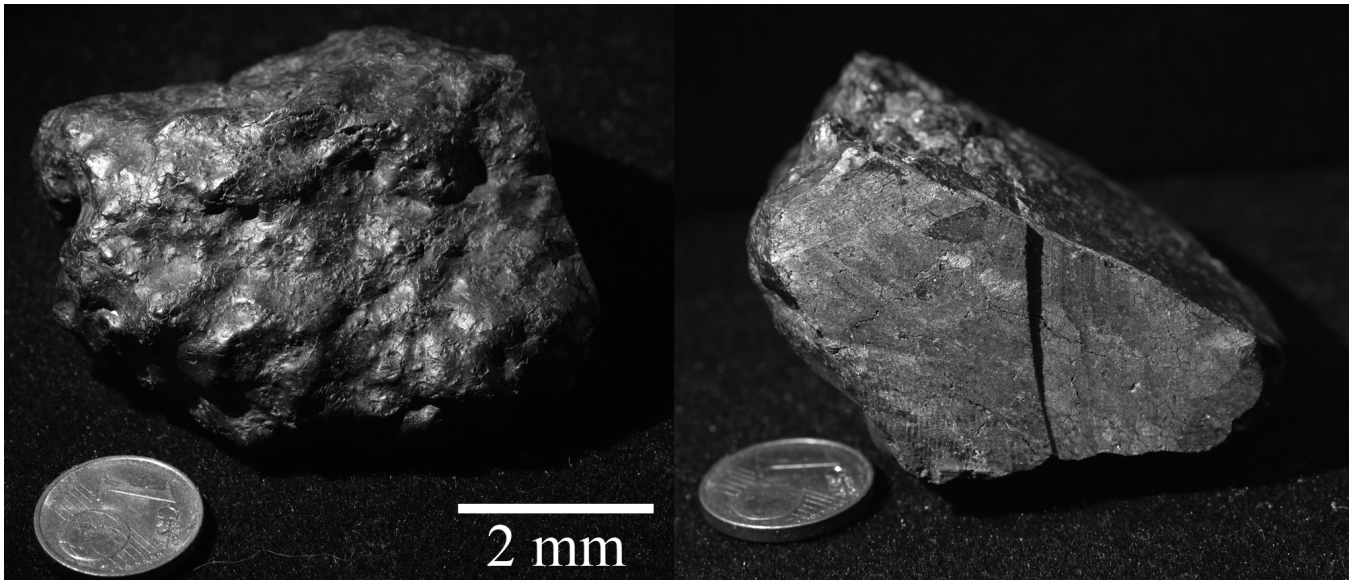

Fig. 1. Photomicrograph of the new ureilite UAE 001. Left: Fusion crust covering the entire meteorite. Right: First cut of the ureilite.

theory diamond formed by impact shock during excavation of the meteorite from its parent body. Arguments in favour of this theory are: (i) diamond in ureilites show a "pronounced crystallographic orientation" supporting shock formation over formation by high gravitational pressure (Lipschutz 1964); (ii) Bischoff et al. (1999) found a correlation between shock stage—obtained from olivines—and the occurrence of diamond, although they did not find a correlation between the abundance of diamond and the shock levels of their host ureilites; (iii) Nakamuta and Aoki (2000) found that C-rich grains associated with diamond have small basal spacings, similar to the basal spacing of compressed graphite. The latter are the precursors of diamond when graphite is directly converted to diamond at high pressures and temperatures. 2) The second, less prevalent theory argues for a nebular vapor-growth origin of diamond. The arguments for this theory are: (i) the Ar-concentration difference between graphite and diamond in ureilites is similar to the difference found in the laboratory when producing chemical vapor deposition (CVD) diamond (Fukunaga et al. 1987); (ii) noble gas distribution between graphite and diamond produced by vapor-growth experiments are identical to what is found in ureilites (Matsuda et al. 1991); (iii) the noble gas inventory of the shock-produced diamond formed in the laboratory experiments is different from the observed one in ureilite diamond (Matsuda et al. 1995); (iv) the uniform $\delta^{15}N$ among diamond grains of different ureilites, but highly diverse $\delta^{15}N$ of other ureilite components do not suggest a genetic link between C-rich material and diamond grains (Rai et al. 2002, 2003); (v) the full width at half maximum (FWHM) of Raman bands of ureilite diamond do not match the FWHM of shocked diamond (Miyamoto et al. 1988, 1989; Miyamoto 1998).

In this study, we characterize diamond and graphite in UAE 001 using in situ X-ray diffraction and micro-Raman technique to further constrain their origin.

TECHNIQUE

Two thin sections of UAE 001 were studied by optical microscopy and analyses for mineral compositions using a JEOL 8900RL electron microprobe (EMP). The accelerating voltage was set to 15 kV and the beam current to 20 nA. The ZAF-algorithm was used for correction. The following 9 elements have been measured (standards and detection limits in wt% in brackets): Si (clinopyroxene, 0.049), Ti (rutile, 0.033), Al (corundum, 0.013), Cr (eskolaite, 0.044), Fe (olivine, 0.042), Mn (rhodonite, 0.034), Ni (bunsenite, 0.043), Mg (periclase, 0.047), Ca (clinopyroxene, 0.026), Na albite, 0.088), K (orthoclase, 0.026). Backscattered electron (BSE) images were taken with the microprobe.

For X-ray fluorescence (XRF) analysis, a sample of the meteorite was thoroughly ground in an agate mortar and the resulting powder was dried in an evacuated desiccator for approximately 48 hours. Two aliquots of 120 mg have been weighed and mixed with 3 mL aqua regia in a Teflon (R) beaker and heated for 2 hours on a hotplate. The residual acid was evaporated within six hours. The dry residuum was mixed with 3.6 g of Spectromelt (R) for preparation of fused beads according to the procedure described in Wolf and Palme (2001). All analyses were performed on a Philips PW 2400 XRF spectrometer. For calibration, a special set of ultramafic geostandards doped with different amounts of FeNi metal (iron meteorite Tocopilla) was used. This calibration set gives a linear correlation between count rates and concentrations within the typical concentration range of meteorites. Furthermore, the alpha correction factors are

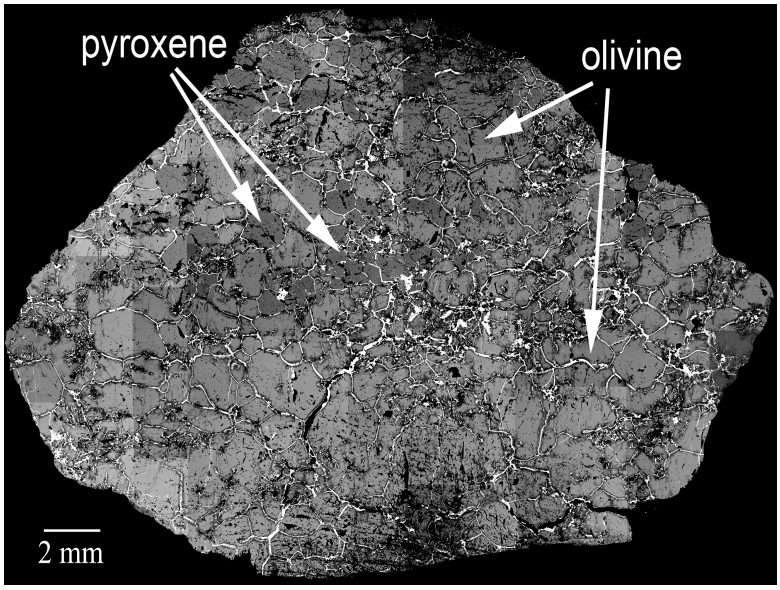

Fig. 2. Backscattered electron photomosaic of the studied ureilite thin section. White spots are Pb remnants from polishing.

small compared to other methods. The instrumental setup, detection limits, and analytical errors were similar to those described in Wolf and Palme (2001).

The diamond grains were studied in situ on two thin sections using Raman microprobe analysis. Measurements were done by means of a Jobin Yvon (Horiba) LabRam HR800 system. This notch filter-based spectrometer was equipped with an Olympus BX41 microscope, a grating with 1800 grooves per mm, and a Si-based charge-coupled device (CCD) detector. Spectra were excited with the He-Ne 632.8 nm emission (3 mW). With the Olympus 100 objective, the lateral resolution was better than 1.5 μm. The wave number accuracy was 0.5 cm^{-1} and the spectral resolution was 0.8 cm^{-1}. Measured FWHMs were corrected for the system's apparatus functions (i.e., spectral resolution with which a measurement was done) using the formula of Irmer (1985).

In situ XRD-measurements have been performed on the same two thin sections of UAE 001 as the micro-Raman studies. The XRD measurements were performed on beamline ID18F (Somogyi et al. 2003) of the European Synchrotron Radiation Facility (ESRF) The X-ray beam was monochromatized to 28 keV with a fixed-exit double Si(111) crystal monochromator ($\Delta E/E \sim 10^{-4}$). The beam was focused to a 1.5*4.5 μm^2 spot (vertical*horizontal) with Compound Refractive Lenses (CRL; Snigirev et al. 1996) made of 112 individual Al lenses. The spot size in the focal plane was determined by the knife-edge optical method using a thin gold test object. The intensity of the focused beam was in the order of 10^{10} photons/second during all the experiment. An optical microscope was used to align the sample at 45° from the beam in its focal plane. The sample position was controlled with a remote-controlled four axis (x, y, z, α) sample stage. XRD images were acquired using a MARCCD 165 diffraction camera placed at 100.942 mm behind the sample.

RESULTS

Petrography and Chemical Composition

Figure 2 shows a BSE photomosaic of one of the analyzed thin sections. The meteorite has an equigranular appearance, with no foliation or elongated silicates are visible. It is an ultramafic rock, displaying the typical, coarse-grained, equilibrated ureilite texture, except for the missing foliation (Goodrich 1992; Mittlefehldt et al. 1998, 2004). The bulk composition tabulated in Table 1 is typical of ureilites (e.g., Koblitz 2006 and references therein). Anhedral, ~1–3 mm large olivines and pigeonites occur as major phases, with a modal abundance of ~90 vol% olivines and ~10 vol% pigeonite. No plagioclase, individual metal grains, sulfide or pyroxene other than pigeonite was found. Olivine grain boundaries often meet in triple junctions with 120° angles. Analysis of 71 olivine grains gave a narrow range of $Fo_{79.8–81.8}$ and a mean of $Fo_{80.4}$, MnO = 0.43, Cr_2O_3 = 0.71 and CaO = 0.38 wt% (Table 2). The cores of the olivines are homogenous, but Mg increases toward olivine borders, forming ~10–100 μm thick rims with up to $Fo_{96.1–96.8}$ (Fig. 3). Enstatite is in some cases found in association with these rims (Fig. 3). Numerous tiny, Ni-poor and Fe-rich droplets occur in the Fo-rich rims. Analytical sums of these Fe-rich particles are far below 100 wt%, indicating that the original metal particles are now Fe-hydroxide. Some olivines show deformation lamellae, sometimes kink bands, undulatory extinction and few have subgrain boundaries, indicating medium shock level (Mittlefehldt et al. 1998).

Table 1. Bulk chemical composition of UAE 001 obtained using XRF.

		UAE 001
SiO_2	wt%	34.65
TiO_2	wt%	0.012
Al_2O_3	wt%	0.28
Fe_2O_3	wt%	20.70
MnO	wt%	0.38
MgO	wt%	35.10
CaO	wt%	0.83
Na_2O	wt%	0.017
K_2O	wt%	0.017
P_2O_5	wt%	0.087
V	ppm	77
Cr	ppm	4500
Co	ppm	262
Ni	ppm	1184
Zn	ppm	207
Sr	ppm	108
Total		92.70

Table 2. Chemical composition of olivines (ol) and pyroxenes (px).

	Mean ol core	Ol rim	Ol rim	Mean px
SiO_2	39.47	42.63	42.37	55.69
TiO_2	0.04	0.04	0.08	0.09
Al_2O_3	0.03	0.03	0.02	0.66
Cr_2O_3	0.71	0.47	0.59	1.10
FeO	18.04	3.82	3.18	10.58
MnO	0.43	0.37	0.58	0.41
MgO	41.62	53.29	54.47	27.11
CaO	0.38	0.30	0.25	4.57
Na_2O	<.09	<.09	<.09	<.09
Total	100.72	100.95	101.53	100.23
Fo	80.440	96.138	96.830	
En				74.619

Mean value of olivine (ol) and pyroxene (px) calculated from 71 and 28 analyses, respectively. Forsterite and enstatite contents are calculated from cations per formula unit.

Analysis of 28 pigeonite grains gave a range of $En_{73.9–75.2}$, $Fs_{15.5–16.9}$, $Wo_{8.8–9.5}$, MnO = 0.41, Cr_2O_3 = 1.10 and CaO = 4.57 wt% (Table 2). Pigeonite rims are generally similar to their cores. Both olivine and pyroxene compositions are typical of ureilites (Mittlefehldt et al. 1998, 2004). Vein material interstitial to silicate grains consists of Fe-rich material. Analytical sums are highly variable and again far below 100 wt%, indicating Fe-hydroxide as main vein constituent.

A distinct feature of this new ureilite compared to known ureilites are the relatively large diamond grains with up to tens of μm in size (Fig. 4). The diamonds occur embedded in graphite areas (up to several hundred μm long) that are interstitial to olivine and pyroxene (Fig. 4). Under the optical microscope graphite appears either as long bent books or is polycrystalline (El Goresy, personal communication).

Micro-Raman Analyses of Diamond

Micro-Raman, used as a fingerprinting technique, allows in situ identification of minerals and their polymorphs in thin sections. In addition, this technique can provide valuable information about the structure and short-range order of minerals. For instance, Sato (1984) pointed out that the type of diamond formation leaves a diagnostic signature in the FWHMs of the main diamond Raman band, which in turn can be used to identify the origin of diamond. We found abundant diamond grains interstitial to silicate grains in the thin section (Fig. 4) and measured the FWHM of LO=TO Raman bands of 33 diamond grains. Typical Raman spectra are shown in Fig. 5. The FWHMs of diamond grains in UAE 001 lie in the range between 4 and 13 cm^{-1}, with a maximum around 7 cm^{-1} (Fig. 6). Band positions and FWHMs are inversely correlated, i.e., positions are shifted to lower wave numbers with increasing FWHM, and vice versa. Note that in the experiments, the laser power (3 mW measured behind the microscope objective) was well below the threshold for any spectral changes due to local upheating as caused by heavy light absorption. In addition, the excitation was uniform for all individual measurements. Therefore, analytical artifacts such as band shift due to different excitation energies (Zhao et al. 1998; Zouboulis and Grimsditch 1991) can be excluded.

In Situ X-Ray Diffraction Analyses of Diamond

Areas containing large diamond grains were chosen for in situ X-ray analysis. We performed line scans and maps in about 40 different locations of both UAE 001 thin sections. All diamond was the cubic polymorph, no hexagonal lonsdaleite was found. Only one or two single spots (not continuous lines or arcs) were observed on 2D images, indicating that the size of individual diamond subgrains of a large polycrystalline diamond grain observed with the optical microscope must be similar or even larger than the spot size, i.e., >5 μm. The diamond polishing agent used in the final polishing had a grain size of <1 μm, much smaller than the diamond grain size determined using XRD. This size difference excludes that we accidentally measured polishing diamond. Graphite occurs as normal (d002 ~3.35 Å) and as compressed (d002 ~3.3Å) graphite (Nakamuta and Aoki 2000; Irifune et al. 2004). Figure 7 shows a typical diffractogram of diamond, graphite and compressed graphite found in UAE 001. The diamond (111) line is slightly shifted to a lower d-value of 2.046 Å.

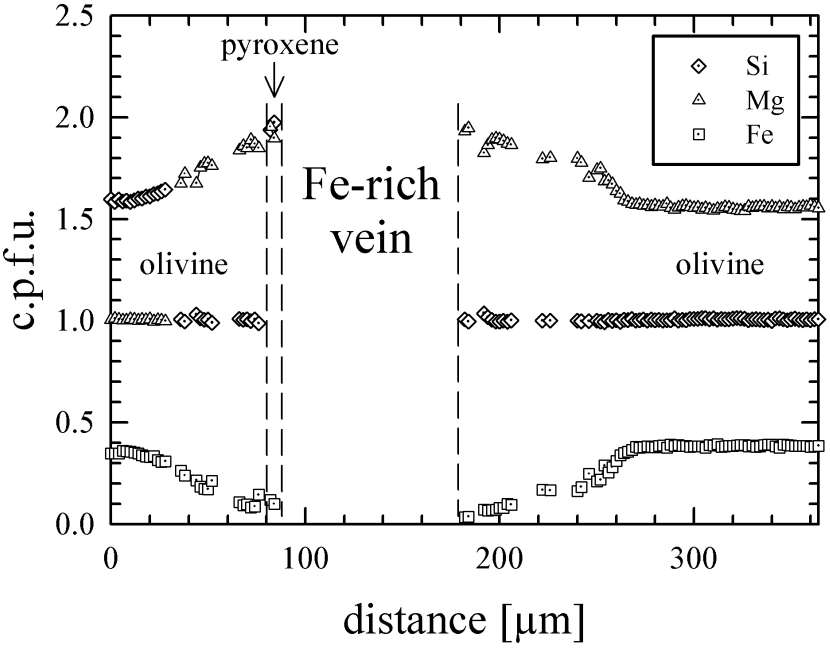

Fig. 3. Line profile across two olivine borders adjacent to an altered Fe-hydroxide filled vein. The left olivine has a thin layer of pyroxene on its rim. Si and Mg data points for pyroxene overlap. c.f.p.u. = cation per formula unit.

DISCUSSION

UAE 001 belongs to the typical ureilite main group. The mean #mg number of $Fo_{80.4}$ of the olivines is close to the peak of ureilites that is Fo_{79} (Goodrich 1992; Mittlefehldt et al. 1998). The increase in Fo content of olivines and the occurrence of tiny Fe-rich droplets in their rims is commonly explained by secondary reduction. The enstatite found at the border of some olivines supports this reduction process, as pyroxene can be formed by the olivine reduction reaction:

$$Mg_{2-x}Fe_xSiO_4 \rightarrow (1-x)\cdot Mg_2SiO_4 + x\cdot MgSiO_3 \quad (1)$$
$$+ x\cdot Fe + \frac{x}{2}\cdot O_2 \text{ with } x = \{0\ldots1\}$$

The veins interstitial to the silicate grains are mainly filled with Fe-hydroxide. This is typical of terrestrial alteration, indicating that UAE 001 was exposed to weathering for a long period of time in the desert.

The optical microscope and XRD studies strongly support an impact origin of the diamonds: (i) XRD studies revealed the presence of compressed graphite (Fig. 7), which is the first step of converting graphite into diamond during pressure increase (Nakamuta and Aoki 2000). (ii) Optical observations revealed primary graphite occurring as large books and polycrystalline secondary graphite. The latter forms from the back transformation of shock-produced diamond (El Goresy, personal communication). The preservation of shock produced diamond requires well-defined conditions like quenching from high temperature (e.g., DeCarli et al. 2002). The coexistence of diamond and secondary graphite illustrate the locally heterogeneous P and T conditions with hotspots for diamond formation (DeCarli et al. 2002) as should be expected during an impact. (iii) Diamonds in UAE 001 are often accompanied by large areas of graphite (several hundred μm). CVD produced diamonds are usually accompanied by only small amounts of graphite, although a main reason for this is that graphite production is suppressed by a nearly pure H_2-atmosphere (e.g., Yarnell 2004). However, CVD production has a vast parameter space (e.g., Fabisiak et al. 2006) and diamond might also be accompanied by larger amounts of graphite. We conclude from these features that the diamonds in UAE 001 formed as response to impact and not by a CVD process.

Another explanation has then to be found for the broadened FWHM of the diamonds that are in the range of CVD diamonds (Fig. 8). The Raman spectrum of diamond is characterized by one main first-order band, which is usually referred to as LO=TO mode (due to the high symmetry, longitudinal and transversal optical vibrations are degenerate and appear as one single band at ~1332 cm^{-1}). In the case of well-ordered diamond single-crystals, this band has a FWHM of about 1.7 cm^{-1} (Solin and Ramdas 1970). The LO=TO Raman bands obtained from diamonds in UAE 001, in contrast, have FWHMs in the range 4–13 cm^{-1}. Previous FWHMs of Raman bands of diamond have been measured (i) in the ALH 77257, Y-790981 and Y-791538 ureilites by e.g., Miyamoto et al. (1989) and Miyamoto (1998) who found FWHM between ~5 and ~15 cm^{-1}; (ii) in the Canyon Diablo meteorite by Miyamoto (1998) who found FWHM between

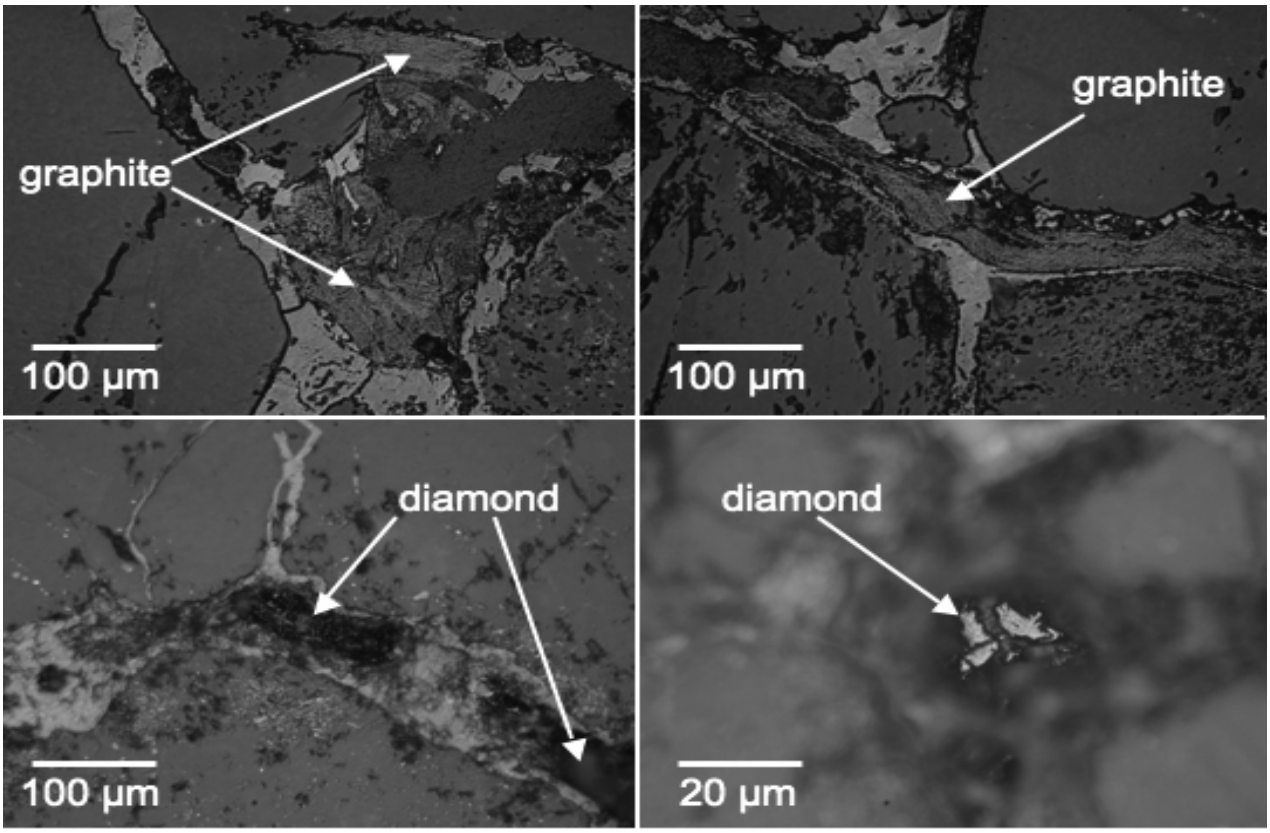

Fig. 4. Reflected light images showing typical graphite and diamond in UAE 001.

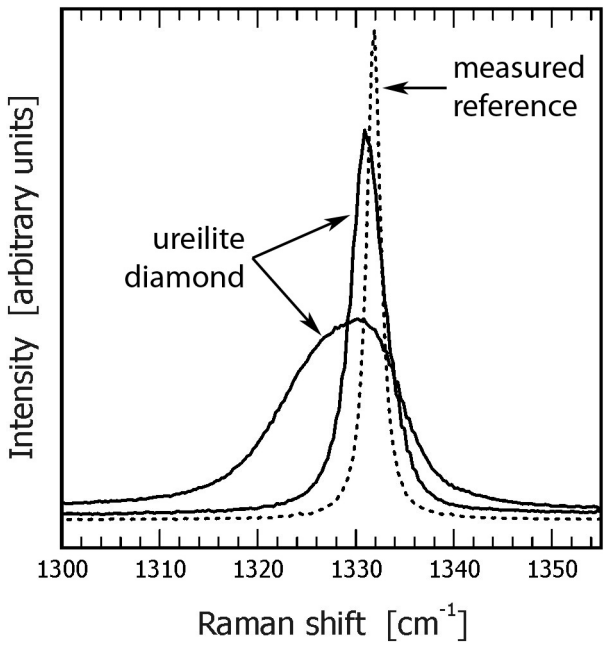

Fig. 5. Two Raman spectra obtained from diamond in the ureilite UAE 001 (solid lines) in comparison with the measured reference spectrum of a large diamond single-crystal from the Earth's mantle (dotted line; intensity ×0.25). Note that the main band in the spectra of ureilite diamond shows an increased FWHM and is shifted to lower wave numbers.

25 and 117 cm^{-1} and by Heymann (1989) who found a FWHM of 7 ± 2 cm^{-1}; and (iii) in diamond found in shocked gneisses associated with the Ries crater in Germany by El Goresy et al. (2001) yielding a FWHM of 4.5 cm^{-1} and by Lapke et al. (2000) yielding a FWHM between 73 and 170 cm^{-1}. Figure 8 displays all these results including our new data together with FWHM of natural (2–3 cm^{-1}), experimentally shock produced (10–120 cm^{-1}) and vapor grown CVD diamond (3–25 cm^{-1}; dashed areas; Miyamoto 1998 and references therein). The fields of shock produced and CVD diamond overlap between 10 and 25 cm^{-1}.

The nature of the FHWM found in ureilite diamond is controversial (e.g., Miyamoto et al. 1988, 1989 and Heymann 1989). The similar FWHM of diamond in ureilites and CVD produced diamonds (Fig. 8) lead Miyamoto et al. (1988, 1989) to the conclusion that a CVD origin of ureilite diamonds should be considered seriously. Heymann (1989) rebutted that the FWHM of diamonds should be interpreted cautiously. He reports a Raman spectrum of one diamond in the Canyon Diablo meteorite that is interpreted to have formed as result to the impact. This diamond has a FWHM of 7 ± 2 cm^{-1}, in the range of CVD diamonds and not >10 cm^{-1}, as should be expected for shock produced diamonds. However, Miyamoto (1998) also studied diamonds in the Canyon Diablo meteorite and found FWHMs solely in the range between 25 and 117 cm^{-1}, in accordance with shock-produced

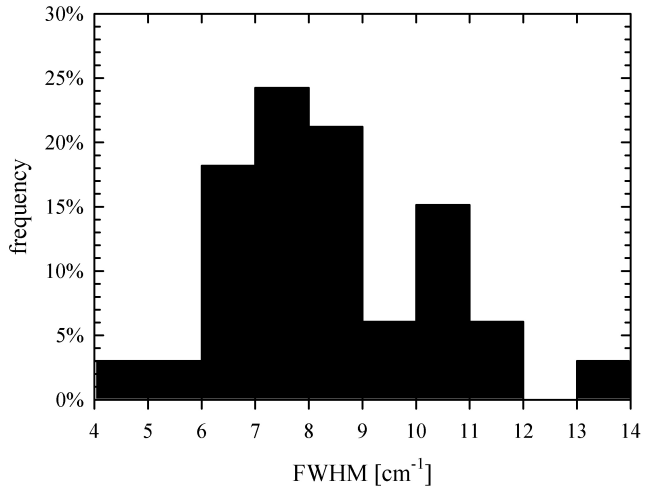

Fig. 6. Histogram showing the LO=TO Raman band full widths at half maximum (FWHM) of 33 diamonds measured in UAE 001.

diamonds. Miyamoto (1998) suggests that different "degree and duration of shock pressure" might have lead to different FWHM in different samples. However, these conflicting results show that Raman peak shape, shift and width is not a simple diagnostic tool for the origin of diamonds, as different features of diamond can produce a broadening in the FWHM.

It is well known that the diamond LO=TO band may broaden as a result of lattice distortion (i.e., minute amounts of trace elements, internal strain) and elevated pressures acting on diamond (Sharma et al. 1985; Nasdala et al. 2005). Band broadening due to remnant pressure, however, can be excluded in our case because (i) surfaces of polished samples were analyzed. The exposure of micro-areas to the surface is likely to result in nearly complete pressure relaxation, and (ii) pressure-induced FWHM increase of well-ordered diamond is always accompanied by an increased LO=TO Raman shift, whereas we observed lower Raman shifts of more broadened bands (Fig. 5). The presence of lonsdaleite can produce a downshift of the Raman band (e.g., Miyamoto et al. 1993), but our XRD-analyses have not shown any lonsdaleite associated with the diamond. Band broadening can also be the result of small grain sizes. This feature is typical of diamond grains with sizes on the order of the excitation wavelength, i.e., smaller than ~2 μm. This effect has been measured and is small. For example grains with a size range between 0 and 2 μm give a line width of 3.1 cm^{-1} and grains with a size range of 0 to 0.1 μm give a line width of 3.8 μm (Yoshikawa et al. 1993; see also Salje 1973). These numbers are well below the FWHMs we measured for the diamonds in UAE 001. Yoshikawa et al. (1993) also performed calculations and predicted that line broadening can result in FWHM of up to 38 cm^{-1} for 5 nm sized grains. Yoshikawa et al. (1993) also tried to obtain Raman spectra from a diamond powder with diamond grains of this size, but failed and stated that it might be not possible to obtain Raman spectra from such small crystallites. We determined the size of individual diamond grains as >5 μm, therefore the band broadening cannot be the result of diamond grain size. El Goresy et al. (2001) described individual diamond subgrains in polycrystalline diamond from the Ries crater as <1 μm, however, the Raman band of these diamond still have a FWHM of only 4.5 cm^{-1}. Koeberl et al. (1997) deduced sizes for individual diamond microcrystals from the Popigai crater as around 1 μm. Langenhorst et al. (1999) found an average size of as low as 28 nm for impact diamonds from the Lappajärvi crater. The different crystallite sizes of impact diamonds are probably the result of different shock conditions among different impact events or at different locations of a single impact event.

Broad FWHM are also the result of lattice disorder, as it has been similarly observed from diamond that formed by either vapor-growth or shock-compression (e.g., Derjaguin et al. 1968; Langenhorst et al. 1999; Moroz et al. 2000). Line broadening of diamond FWHM is commonly and widely used as quality measure for CVD diamonds (e.g., Fabisiak et al. 2006 and references therein). The narrower the FWHM, the better the quality, i.e., the better ordered the crystal is. Although it is noted that Miyamoto (1998) points out that it is not really defined what the degree of ordering exactly means.

We therefore suggest that the broadening of diamond Raman bands maybe explained by prolonged shock duration during an impact. It was pointed out by e.g., Melosh (1989) that the duration of the shock during impact is sometimes underestimated. Shocks produced in the laboratory are usually in the order of μs, whereas impact shocks are 10^3–10^6 times longer, in the order of ms to a few s (DeCarli et al. 2002). It might be possible that the FWHM of Raman bands of diamond narrow with prolonged duration of high pressure, i.e., the degree of ordering in the diamond lattice might increases over time towards the well-ordered lattice of diamond that formed under lithostatic pressure which has small FWHM (Fig. 8). We observed a shift in the 2.06/220 diamond line. This might indicate a still slightly disordered diamond lattice causing the broadening of the diamond Raman band. In this case, the FWHM of Raman bands of ureilite diamond would represent a transitional signal between diamond formed by shock and lithostatic pressure. Raman analyses would, in this case not be diagnostic of the origin of diamond. On the other hand, if a shock origin of diamond is beyond doubt, diamond would provide a measure for shock/impact duration. The large FWHM found in Canyon Diablo and some Ries crater diamond would indicate shorter and the smaller FWHM of ureilite diamond would indicate longer shock duration. The even smaller FWHM of diamonds reported by El Goresy et al. (2001) would also indicate longer shock duration for the Ries crater impact. The hypothesis of a change of the FWHM of shock-produced diamond with exposure to high pressure can potentially be tested by experimental studies with longer shock duration.

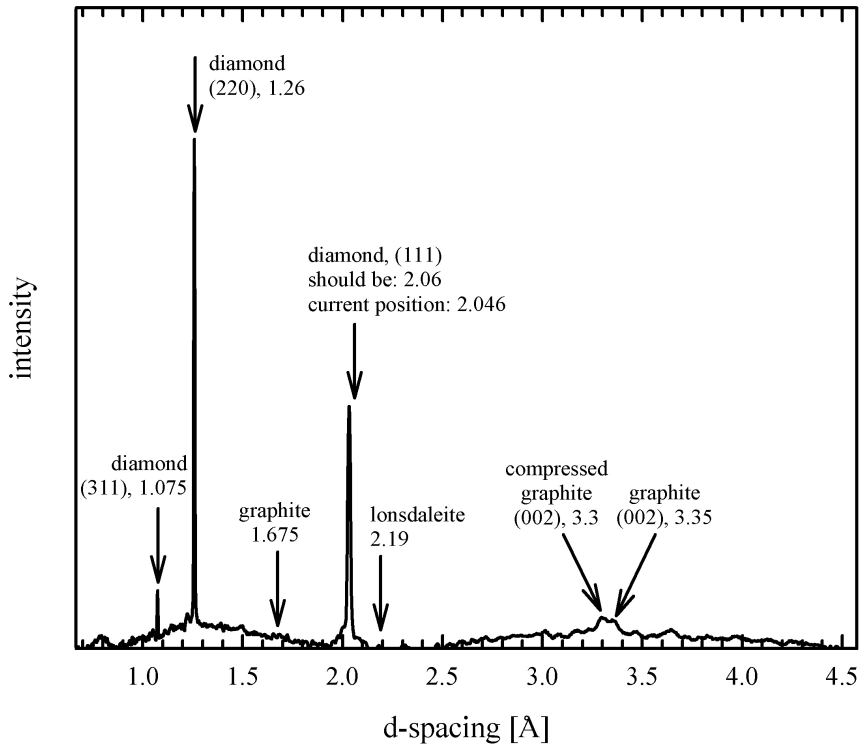

Fig. 7. Typical XRD spectra of a diamond. The line at 2.06 is slightly shifted to a lower value of 2.046. This shift in the diamond lattice might be a reason for the broadening of the diamond Raman bands. Expected position of lonsdaleite indicated, but we did not find any of this hexagonal diamond polymorph.

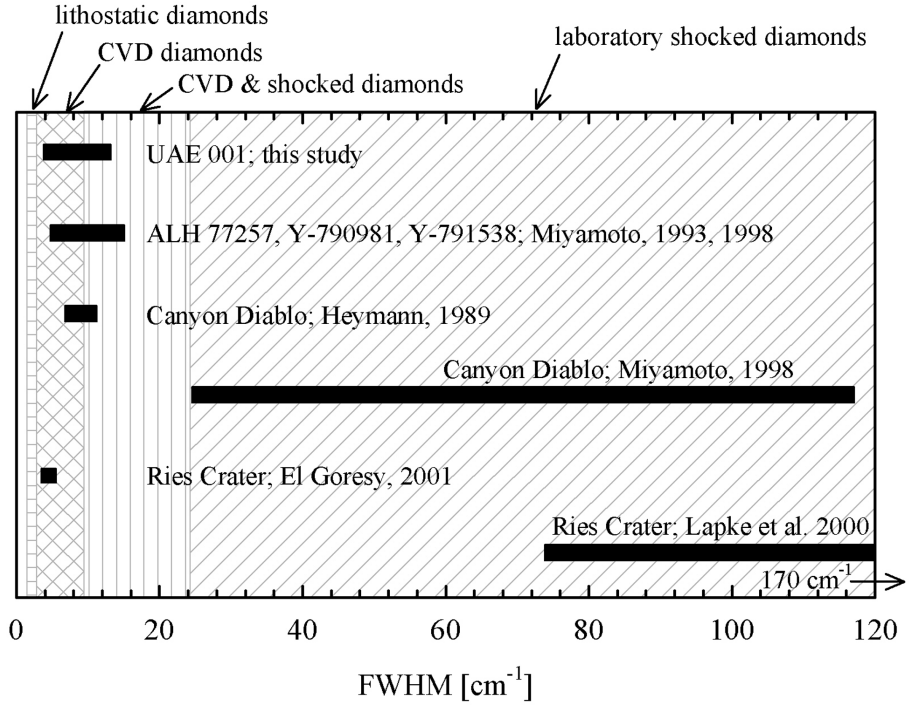

Fig. 8. Raman band full widths at half maximum (FWHM) of diamond grains of different ureilites and diamond grains associated with impact craters. The dashed areas reflect Raman band FWHM of diamond of various origin as known from natural occurrence and/or experiments (Miyamoto 1998 and references therein).

SUMMARY

This is the first report of a meteorite from United Arab Emirates. UAE 001 is a typical ureilite that contains numerous and unusually large diamonds. Compressed graphite in the vicinity of diamond, the occurrence of polycrystalline secondary graphite, and the large amounts of graphite accompanying the diamond are best explained by the formation during a shock event. The secondary graphite requires the production of diamond during the impact event. Slightly variable conditions during the impact are sufficient to prevent some diamond from back transformation to graphite. We therefore suggest that all diamond in ureilites formed as response to shock. If this is accepted, then the small FWHM of diamond Raman bands in UAE 001 relative to the much larger FWHM of laboratory produced shock diamonds might be explained by prolonged shock duration, during which diamond starts converting from a highly unordered (large FWHM) towards a more well-ordered (smaller FWHM) state.

Acknowledgments—We are grateful for samples provided by H. Kallweit and UAE officials. Thanks are due to H. Palme for helpful comments and suggestions on the manuscript, and to R. Kleinschrodt and A. Bischoff for assistance with optical microscopy. D. C. Hezel and A. Simionovici thank the ESRF for a travel and measurement grant and Gema Martinez-Criado, Holger Witsch and ESRF staff for their help during measurements. We thank M. Miyamoto, J. Matsuda, S. Singletary, D. Heymann and T. Bunch for constructive reviews or comments on an earlier version of this manuscript. A. El Goresy is thanked for useful reviews. We also thank C. A. Goodrich for comments and editorial handling. K. Fabisiak is thanked for helpful discussions about CVD and impact diamonds and their Raman signals. We are indebted to R. Hollerbach for the photographs of the ureilite shown in Fig. 1, and to P. Garcia for preparing an excellent thin section of the ureilite sample. Thanks to Sara Russell and Caroline Smith for discussions.

Editorial Handling—Dr. Cyrena Goodrich

REFERENCES

Bischoff A., Goodrich C. A., and Grund T. 1999. Shock-induced origin of diamonds in ureilites (abstract #1100). 30th Lunar and Planetary Science Conference. CD-ROM.

Connolly H. C. Jr., Zipfel J., Folco L., Smith C., Jones R. H., Benedix G., Righter K., Yamaguchi A. Chennaoui H. A., and Grossman J. N. 2007. The Meteoritical Bulletin, No. 91, 2007, March. *Meteoritics & Planetary Science* 42:413–466.

Derjaguin B. V., Fedoseev D. V., Lukyanovich V. M., Spitsyn B. V., Ryabov V. A., and Lavreutyev A. V. 1968. Filamentary diamond crystals. *Journal of Crystal Growth* 2:380–384.

DeCarli P. S., Jones A. P., and Price G. D. 2002. Laboratory impact experiments and calculations versus natural impact events. In *Catastrophic events and mass extinctions: Impacts and beyond,* edited by Koeberl C. and MacLeod K. G. GSA Special Paper 356. Boulder, Colorado: Geological Society of America. 746 p.

El Goresy A., Gillet P., Chen M., Künstler F., Graup G., and Stähle V. 2001. In situ discovery of shock-induced graphite-diamond phase transition in gneisses from the Ries crater, Germany. *American Mineralogist* 86:611–621.

Fukunaga K., Matsuda J., Nagao K., Miyamoto M., and Ito K. 1987. Noble-gas enrichment in vapor-growth diamonds and the origin of diamonds in ureilites. *Nature* 328:141–143.

Fabisiak K., Banaszak A., Kaczmarski M., and Kozanecki M. 2006. Structural characterization of CVD diamond films using Raman and ESR spectroscopy methods. *Optical Materials* 28:106–110.

Goodrich C. A. 1992. Ureilites: A critical review. *Meteoritics* 27: 327–352.

Heymann D. 1989. Is the width of the Raman line of diamond diagnostic for the origin of diamonds in meteorites? Comment on "Raman spectra of ureilite diamonds" by Miyamoto M., Nishimura Y., Matsuda J., and Ito K. *Geochimica et Cosmochimica Acta* 53:3059–3060.

Hezel D. C., Schönbeck Th., and Nasdala L. 2006. A ureilite (UAE 001) from United Arab Emirates (abstract). *Meteoritics & Planetary Science* 41:A207.

Irifune T., Kurio A., Sakamoto S., Inoue T., Sumiya H., and Funakoshi K. 2004. Formation of pure polycrystalline diamond by direct conversion of graphite at high pressure and high temperature. *Physical Earth and Planetary Interiors* 143–144: 593–600.

Irmer G. 1985. Zum Einfluß der Apparatefunktion auf die Bestimmung von Streuquerschnitten und Lebensdauern aus optischen Phononenspektren. *Experimentelle Technik der Physik* 33:501–506.

Koeberl C., Masaitis V. L., Shafranovsky G. I., Gilmour I., Langenhorst F., and Schrauder M. 1997. Diamonds from the Popigai impact structure, Russia. *Geology* 25:967–970.

Koblitz J. 2006. MetBase 7.2. CD-ROM.

Langenhorst F., Shafranovsky G. I., Masaitis V. L., and Koivisto M. 1999. Discovery of impact diamonds in a Fennoscandian crater and evidence for their genesis by solid state transformation. *Geology* 27:747–750.

Lapke C., Schmitt R. T., Kenkmann T., and Stöffler D. 2000. Raman microspectrometry of impact diamonds from the Ries crater, Germany (abstract). *Meteoritics & Planetary Science* 35:A95.

Lipschutz M. E. 1964 Origin of diamonds in the ureilites. *Science* 143:1431–1434.

Matsuda J., Fukunaga K., and Ito K. 1991. Noble gas studies in vapor-growth diamonds: Comparison with shock-produced diamonds and the origin of ureilites. *Geochimica et Cosmochimica Acta* 55:2011–2023.

Matsuda J., Kusumi A., Yajima H., and Syono Y. 1995. Noble gas studies in diamonds synthesized by shock loading in the laboratory and their implications on the origin of diamonds in ureilites. *Geochimica et Cosmochimica Acta* 59:4939–4949.

Melosh H. J. 1989. *Impact cratering: A geologic process*. Oxford University Press. 245 p.

Mittlefehldt D. W. 2004. Achondrites. In *Meteorites, comets and planets*, edited by Davis A. M. Treatise on Geochemistry, vol. 1. Oxford: Elsevier-Pergamon. pp. 291–324.

Mittlefehldt D. W., McCoy T. J., Goodrich C. A., and Kracher A. 1998. Non-chondritic meteorites from asteroidal bodies. In *Planetary materials*, edited by Papike J. J. Reviews in Mineralogy and Geochemistry, vol. 36. Washington, D. C.: Mineralogical Society of America. 398 p.

Miyamoto M. 1998. Micro-Raman spectroscopy of diamonds in the Canyon Diablo iron meteorite: Implication for the shock origin. *Antarctic Meteorite Research* 11:171–177.

Miyamoto M., Takase T., and Mitsuda Y. 1993. Raman spectra of various diamonds. *Mineralogical Journal* 16:246–257.

Miyamoto M., Matsuda J., and Ito K. 1988. Raman spectroscopy of diamond in ureilite and implication for the origin of diamond. *Geophysical Research Letters* 15:1445–1448.

Miyamoto M., Nishimura Y., Matsuda J., and Ito K. 1989. Raman spectra of ureilite diamonds (abstract). 20th Lunar and Planetary Science Conference. pp. 709–710.

Moroz T. N., Fedorova E. N., Zhmodik S. M., Mironov A. G., Rylov G. M., Ragozin A. L., Afanasyev A. D., and Zaikovsky V. I. 2000. Investigation of various carbon modifications by means of Raman spectroscopy. *Chemistry for Sustainable Development* 8: 43–47.

Nakamuta Y. and Aoki Y. 2000. Mineralogical evidence for the origin of diamond in ureilites. *Meteoritics & Planetary Science* 35:487–493.

Nasdala L., Hofmeister W., Harris J. W., and Glinnemann J. 2005. Growth zoning and strain patterns inside diamond crystals as revealed by Raman maps. *American Mineralogist* 90:745–748.

Rai V. K., Murty S. V. S., and Ott U. 2002. Nitrogen in diamond-free ureilite Allan Hills 78019: Clues to the origin of diamond in ureilites. *Meteoritics & Planetary Science* 37:1045–1055.

Rai V. K., Murty S. V. S., and Ott U. 2003. Nitrogen components in ureilites. *Geochimica et Cosmochimica Acta* 67:2213–2237.

Sato Y. 1984. Characterization of diamond by Raman spectroscopy. *Research on diamond.* Research Report of the National Institute in Research of Inorganic Materials, Tsukuba, vol. 39. pp. 50–56.

Sharma S. K., Mao H. K., Bell P. M., and Xu J. A. 1985. Measurement of stress in diamond anvils with micro-Raman spectroscopy. *Journal of Raman Spectroscopy* 16:350–352.

Salje E. K. H. 1973. Experimentelle Untersuchung der Ramanstreuung an Kristallpulvern. *Journal of Applied Crystallography* 6:442–446.

Somogyi A., Drakopoulos M., Vincze L., Vekemans B., Camerani C., Janssens K., Snigirev A., and Adams F. 2003. ID18F: A new micro-X-ray fluorescence end-station at the European Synchrotron Radiation Facility (ESRF): Preliminary results. *X-Ray Spectrometry* 30: 242–252.

Snigirev A., Kohn V., Snigireva A., and Lengeler B. 1996. A compound refractive lens for focusing high-energy X-rays. *Nature* 384: 49–51.

Solin S. A. and Ramdas A. K. 1970. Raman spectrum of diamond. *Physical Review B* 1:1687–1698.

Wolf D. and Palme H. 2001. The solar system abundances of phosphorus and titanium and the nebular volatility of phosphorus. *Meteoritics & Planetary Science* 36:559–571.

Yarnell A. 2004. The many facets of man-made diamonds. *Chemical & Engineering News* 82/05:26–31.

Yoshikawa M., Mori Y., Maegawa M., Katagiri G., Ishida H., and Ishitani A. 1993. Raman scattering from diamond particles. *Applied Physics Letters* 62:3114–3116.

Zhao X.-Z., Cherian K. A., Roy R., and White W. B. 1998. Downshift of Raman peak in diamond powders. *Journal of Materials Research* 13:1974–1976.

Zouboulis E. S. and Grimsditch M. 1991. Raman scattering in diamond up to 1900 K. *Physical Review B* 43:12490–12493.